

Enhanced angiogenesis through controlled release of basic fibroblast growth factor from peptide amphiphile for tissue regeneration

Hossein Hosseinkhani^{a,*}, Mohsen Hosseinkhani^b, Ali Khademhosseini^{c,d},
Hisatoshi Kobayashi^{e,f}, Yasuhiko Tabata^g

^aInternational Center for Young Scientists (ICYS), National Institute for Materials Science (NIMS), Tsukuba, Ibaraki 305-0044, Japan

^bDepartment of Cardiovascular Medicine, Graduate School of Medicine, Kyoto University Hospital, Kyoto 606-8507, Japan

^cHarvard–MIT Division of Health Sciences and Technology, Massachusetts Institute of Technology (MIT), Cambridge, MA 02139, USA

^dCenter for Biomedical Engineering, Department of Medicine, Brigham and Women's Hospital, Harvard Medical School, Cambridge, MA 02139, USA

^eBiomaterials Center, National Institute for Materials Science (NIMS), Tsukuba, Ibaraki 305-0044, Japan

^fInstitute of Biomaterials and Bioengineering, Tokyo Medical and Dental University, Tokyo 113-8549, Japan

^gDepartment of Biomaterials, Field of Tissue Engineering, Institute for Frontier Medical Sciences, Kyoto University, 53 Kawara-cho Shogoin, Sakyo-ku, Kyoto 606-8507, Japan

Received 10 June 2006; accepted 1 August 2006

Available online 22 August 2006

Abstract

In the present study, we hypothesized that a novel approach to promote vascularization would be to create injectable three-dimensional (3-D) scaffolds with encapsulated growth factor that enhance the sustained release of growth factor and induce the angiogenesis. We demonstrate that a 3-D scaffold can be formed by mixing of peptide-amphiphile (PA) aqueous solution with basic fibroblast growth factor (bFGF) suspension. PA was synthesized by standard solid phase chemistry that ends with the alkylation of the NH₂ terminus of the peptide. A 3-D network of nanofibers was formed by mixing bFGF suspensions with dilute aqueous solutions of PA. Scanning electron microscopy (SEM) observation revealed the formation of fibrous assemblies with an extremely high aspect ratio and high surface areas. In vitro and in vivo release profile of bFGF from 3-D network of nanofibers was investigated while angiogenesis induced by the released bFGF was assessed. When aqueous solution of PA was subcutaneously injected together with bFGF suspension into the back of mice, a transparent 3-D hydrogel was formed at the injected site and induced significant angiogenesis around the injected site, in marked contrast to bFGF injection alone or PA injection alone. The combination of bFGF-induced angiogenesis is a promising procedure to improve tissue regeneration.

© 2006 Elsevier Ltd. All rights reserved.

Keywords: Scaffold; Peptide amphiphile; Nanofibers; Self-assembly; Angiogenesis

1. Introduction

Tissue engineering is designed to regenerate natural tissues or to create biological substitutes for defective or lost organs by making use of cells. Considering the usage of cells in the body, it is no doubt that a sufficient supply of nutrients and oxygen to the transplanted cells is vital for their survival and functional maintenance [1]. Without a sufficient supply, only a small number of cells pre-seeded in

the scaffold or migrated into the scaffold from the surrounding tissue would survive. Rapid formation of a vascular network at the transplanted site of cells must be a promising way to provide cells with the vital supply.

This process of generating new microvasculature, termed neovascularization, is a process observed physiologically in development and wound healing [2]. It is recognized that basic fibroblast growth factor (bFGF) functions to promote such an angiogenesis process [2,3]. The growth factors stimulate the appropriate cells (e.g., endothelial cells), to migrate from the surrounding tissue, proliferate, differentiate and assemble into blood vessels [2]. However,

*Corresponding author. Tel.: +81 29 851 3354; fax: +81 29 860 4706.

E-mail address: hossein.hosseinkhani@nims.go.jp (H. Hosseinkhani).

one cannot always expect the sustained angiogenesis activity when these proteins are only injected in the solution form probably because of their rapid diffusion from the injected site. One possible way for enhancing the in vivo efficacy is to achieve its controlled release over an extended time period by incorporating the growth factor in a polymer carrier. If this carrier is biodegraded, harmonized with tissue growth, it will work as a scaffold for tissue regeneration in addition to a carrier matrix for the growth factor release. Some studies have demonstrated that bFGF achieved promoted angiogenesis when used in combination with delivery matrices and scaffold [4–9].

Material design of scaffold for cell proliferation and differentiation is one of the key technologies for tissue engineering. The scaffold should mimic the structure and biological function of native extracellular matrix (ECM) as much as possible, both in terms of chemical composition and physical structure. Native ECM does far more than just provide a physical support for cells. It also provides a substrate with specific ligands for cell adhesion and migration, and regulates cellular proliferation and function by providing various growth factors. It is reasonable to expect that an ECM-mimicking tissue-engineered scaffold will play a similar role to promote tissue regeneration in vitro as native ECM does in vivo. A well-known feature of native ECM structures is the nanoscaled dimensions of their physical structure. In a typical connective tissue, structural protein fibers such as collagen and elastin fibers have diameters ranging from several to several hundred nanometers [10]. The nanoscaled protein fibers entangle with each other to form a non-woven mesh that provides tensile strength and elasticity and laminin, which provides specific binding sites for cell adhesion. Three different approaches toward the formation of nanofibrous materials have emerged: self-assembly, electrospinning, and phase separation [11]. Each of these approaches has a unique set of characteristics, which lends to its development as a scaffolding system. For instance, self-assembly can generate small diameter nanofibers in the lowest end of the range of natural ECM collagen, while electrospinning has only generated large diameter nanofibers on the upper end of the range of natural ECM collagen. Phase separation, on the other hand, has generated nanofibers in the same range as natural ECM collagen and allows for the design of macropore structures. These attempts at an artificial ECM have the potential to accommodate cells and guide their growth and subsequent tissue regeneration. Self-assembly, that is, the autonomous organization of molecules into patterns or substrates without human intervention, are common throughout nature and technology. Self-assembly of natural or synthetic macromolecules produces nanoscaled supramolecular structures and nanofibers. Specifically designed amphiphilic peptides that contain a carbon alkyl tail and several other functional peptide regions have been synthesized and shown to form nanofibers through self-assembly process by mixing cell suspensions in media with dilute aqueous solutions of the peptide amphiphile

[12]. The cations in the cell culture medium play an important role to screen electrostatic repulsion among peptides amphiphile and promote self-assembly. These self-assembled nanofibers have been used recently to study selective differentiation of neural progenitor cells [13]. Nanoscaled fibers produced by self-assembly of peptide amphiphile seem to have great potential application in the field of biomaterials and tissue engineering.

The objective of the present study is to fabricate 3-D networks of self-assembled nanofibers by mixing bFGF suspension with aqueous solution of peptide amphiphile as an injectable carrier for controlled release of growth factors and to demonstrate the feasibility of bFGF release from the 3-D hydrogels in enhancing neovascularization.

2. Materials and methods

Amino acid derivatives, derivatized resins, were purchased from Sowa Trading Co. Inc., Tokyo, Japan. A lyophilized human recombinant bFGF (Mw = 17000, isoelectric point (IEP) = 9.6) was purchased from Kaken Pharmaceutical Co. Ltd., Tokyo, Japan. bFGF solutions at concentrations of 0.04, 0.2, 0.6, and 1 $\mu\text{g}/\mu\text{l}$ were made by using phosphate-buffered saline (PBS) solution (pH 7.4) as diluent solution. Other chemicals were purchased from Wako Pure Chemical Industries Ltd., Osaka, Japan and used as obtained. All water used was deionized with a Millipore Milli-Q water purifier operating at a resistance of 18 M Ω .

2.1. Synthesis of the peptide-amphiphile (PA)

The PA was prepared on a 0.5-mmol scale by using standard fluorenylmethoxycarbonyl chemistry (F-moc) [14] on a fully automated peptide synthesizer (Peptide Synthesizer Model 90, Advanced ChemTech, Inc., KY, USA). The chemical structure of PA contain arginine-glycine-aspartic acid (RGD), a glutamic acid (Glu) residue, four alanine (Ala) and three glycine (Gly) residues (A₄G₃), followed by an alkyl tail of 16 carbons. Peptide prepared has a C-terminal carboxylic acid and was made by using prederivatized Wang resin. Briefly, one equivalent of fluorenylmethoxycarbonyl-Asp-Wang resin was reacted with five equivalents of fluorenylmethoxycarbonyl-Gly-OH, five equivalents of fluorenylmethoxycarbonyl-Arg(PMC)-OH, five equivalents of fluorenylmethoxycarbonyl-Glu(OBu)-OH, 15 equivalents of fluorenylmethoxycarbonyl-Gly-OH, and 20 equivalents of fluorenylmethoxycarbonyl-Ala-OH · H₂O in *N*-methyl-2-pyrrolidone. Deprotection was performed with 25% piperidine/DMF. Couplings were achieved using *N,N*-diisopropylcarbodiimide (DIPCI)/HOBT in molar ratio of 1:1. After the peptide portion of the molecule was prepared, the resin was removed from the automated synthesizer and the N terminus was capped with a fatty acid containing 16 carbon atoms. The alkylation reaction was accomplished by using five equivalents of the palmitic acid. Deprotection and coupling reaction was the same as peptide portion. The reaction was allowed to proceed for at least 6 h after which the reaction was monitored by ninhydrin. The alkylation reaction was repeated until the ninhydrin test was negative.

Cleavage (peptide removal from resin) and the removal of side chain protection groups were performed using 95% trifluoroacetic acid (TFA) with 5% water for 2 h at room temperature. The cleavage mixture and two subsequent TCA washings were filtered into a round-bottom flask. The solution was roto-evaporated to a thick viscous solution. This solution was triturated with cold diethylether. The white precipitation was collected by filtration, washed with copious cold ether, and dried under vacuum. PA obtained was further purified by using high-performance liquid chromatography (HPLC, Model LC-6AD, Shimadzu Co. Kyoto, Japan) in a column of Intersil PREP ODS (20 mm × 250 mm) with an eluent of 0.1% TFA/H₂O and CH₃CN at flow rate of 10 ml/min. PA was characterized by matrix-assisted laser desorption ionization-time-of-flight mass

spectroscopy (MALDI-TOF MS, Model Biflex III, Bruker Daltonics Inc., USA) and were found to have the expected molecular weight.

2.2. Formation of 3-D network of self-assembled PA nanofibers

Formation of 3-D network of self-assembled PA nanofibers was carried out by use of PBS solution (pH 7.4) containing 0.04, 0.2, 0.6, and 1 $\mu\text{g}/\mu\text{l}$ of bFGF. A transparent gel-like solid was formed by mixing of bFGF solution (50 μl) at concentration of 10 μg or higher with 1 wt% PA aqueous solution (50 μl) in a 1:1 volume ratio. Formation of nanofibers strongly depends on the particular chemical structure of PA. PA can self-assemble into sheets, spheres, rods, disks, or channels depending on the shape, charge, and environment. Amphiphiles in which the hydrophilic head group is somewhat bulkier than its narrow hydrophobic tail have been shown to form cylindrical micelles [12]. The PA synthesized here contains a hydrophobic domain of 16 carbons and a hydrophilic domain of A_4G_3 , a Glu residue, and RGD. The Glu residue provides a net negative charge at pH 7.4 for PA, so that a part of positive charge of bFGF molecules can screen electrostatic repulsion among them. Thus, once electrostatic repulsions are screened by electrolytes, the molecules are driven to assemble by hydrogen bond formation and by the unfavorable contact among hydrophobic segments and water molecules.

2.3. Morphological observation

The morphology of self-assembled PA nanofibers was observed with a scanning electron microscope (scanning electron microscopy (SEM), S-2380N; Hitachi, Tokyo, Japan). The sample was obtained by network dehydration and critical point drying of samples caged in a metal grid to prevent network collapse. The dried sample was coated with gold on an ion sputterer (E-1010; Hitachi) at 50 mTorr and 5 mA for 30 s and viewed by SEM at a voltage of 15 kV.

2.4. Estimation of in vitro bFGF release from self-assembled PA nanofibers

In vitro bFGF release assay was performed using a fluorescence spectrophotometer. The intrinsic tryptophan fluorescence was observed from protein solutions at 280 nm excitation and 325 nm emission wavelengths. Both the emission and excitation bands were 5 nm. The bFGF calibration indicated that concentrations up to 100 ng/ml are linear curve fit with a minimum detectable concentration of 5 ng/ml. Self-assembled peptide amphiphile nanofibers was prepared by the similar procedure described above by mixing bFGF solution at concentration of 0.04 $\mu\text{g}/\mu\text{l}$ with 1 wt% PA aqueous solution in a 1:1 volume ratio. The solid gel formed was placed in 30 ml of PBS with gentle stirring at 50 rpm at $37^\circ\text{C} \pm 1^\circ\text{C}$. At predetermined time intervals, 1 ml of the releasing medium was sampled and the same volume of fresh buffer solution was added. The fluorescent intensity of the sample solution was measured by a fluorescent spectrophotometer (F-2000 Fluorescent Spectrophotometer, Hitachi Ltd., Tokyo, Japan, Ex 280 nm/Em 325 nm) and divided by that initially added to obtain the percentage of bFGF released. Then cumulative bFGF release was calculated. Each experiment was carried out independently for six samples.

2.5. Estimation of in vivo degradation of self-assembled PA nanofibers incorporated bFGF

In vivo degradation of self-assembled PA nanofibers was evaluated in terms of the radioactivity loss of ^{125}I -labeled PA incorporating bFGF. PA was radioiodinated by use of ^{125}I -Bolton-Hunter reagent. Briefly, 100 μl of ^{125}I -Bolton-Hunter reagent solution in anhydrous was bubbled with dry nitrogen gas until benzene evaporation was completed. Then, 125 μl of 0.1 M sodium borate-buffered solution (pH 8.5) was added to the dried reagent, followed by pipetting to prepare aqueous ^{25}I -Bolton-Hunter solution. The prepared aqueous solution was impregnated into PA at a

volume of 30 $\mu\text{l}/100\text{ mg}$ of powder PA and was kept at 4°C for 3 h to introduce ^{125}I residues into amino groups of PA. The radioiodinated PA were rinsed with double-distilled water (DDW) by exchanging it periodically at 4°C for 4 days to exclude non-coupled, free ^{125}I -labeled reagent from ^{125}I -labeled PA. When measured periodically, the radioactivity of DDW returned to a background level after 3 days rinse.

For the estimation of in vivo degradation of self-assembled PA nanofibers incorporated bFGF, 50 μl of ^{125}I -labeled PA aqueous solution and 50 μl of bFGF solution (at concentration of 10 μg) were carefully injected separately at the same time into the back subcutis of 5-week-age BALB/c male mice (Shimizu Laboratory Supply Inc., Japan). At 1, 3, 7, 10, 14, 21, and 28 days after injection, the radioactivity of PA injected was measured on a gamma counter (ARC-301B, Aloka Co. Ltd., Tokyo, Japan). Next, the mouse back skin around the injected site was cut into a strip measuring $3 \times 5\text{ cm}^2$ and the corresponding fascia site was thoroughly wiped off with a filter paper to absorb ^{125}I -labeled PA. The radioactivity of the skin strip and the filter paper was measured to evaluate the remaining radioactivity of tissue around the injected site. The ratio of the total radioactivity to the initial radioactivity was expressed as the percentage of remaining activity for PA degradation. Six mice were sacrificed at each time point for in vivo evaluation unless otherwise mentioned.

2.6. Estimation of in vivo bFGF release from self-assembled PA nanofibers

In vivo bFGF release assay was evaluated in terms of the radioactivity loss of ^{125}I -labeled bFGF. The radiolabeling of bFGF was performed according to the method of Greenwood et al. [15]. Briefly, 4 μl of Na^{125}I solution was added to 40 μl of 1 mg/ml bFGF solution containing 5 mM glutamic acid, 2.5 wt% glycine, 0.5 wt% sucrose, and 0.01 wt% Tween 80 (pH 4.5). Then, 0.2 mg/ml of chloramine-T potassium phosphate-buffered solution (0.5 M, pH 7.5) containing 0.5 M sodium chloride (100 μl) was added to the solution mixture. After agitation at room temperature for 2 min, 100 μl of PBS (pH 7.5) containing 0.4 mg of sodium metabisulfate was added to the reaction solution to stop the radioiodination. The reaction mixture was passed through an anionic-exchange column to remove the uncoupled, free ^{125}I molecules from the ^{125}I -labeled bFGF.

For the estimation of in vivo bFGF release, 50 μl of PA aqueous solution and 50 μl of ^{125}I -labeled bFGF were carefully injected separately at the same time into the back subcutis of 5-week-age BALB/c male mice. As a control, 100 μl of ^{125}I -labeled bFGF was subcutaneously injected into the mouse back. The dose of ^{125}I -labeled bFGF was 10 μg for both cases. At different time intervals, the mouse skin including the injected site was taken out and the corresponding fascia site was thoroughly wiped off with a filter paper, as described above to absorb ^{125}I -labeled bFGF. The radioactivity of the PA remained and the skin strip plus the filter paper was measured on a gamma counter and their ratios to the initial radioactivity were expressed as the percentage of remaining activity for in vivo bFGF retention. Six mice were sacrificed at each time point for in vivo evaluation unless otherwise mentioned.

2.7. In vivo assessment of angiogenesis induced by bFGF released from self-assembled PA nanofibers

BALB/c male mice (5 weeks old) were divided into three groups. For group I, control group ($n = 6$), 100 μl of PA aqueous solution was injected into the back subcutis of mice. In group II ($n = 24$), 100 μl of bFGF solutions (at concentrations of 0.08, 0.1, 0.3, and 0.5 $\mu\text{g}/\mu\text{l}$) was injected into the back subcutis of mice ($n = 6$ for each concentration). For group III ($n = 24$), 50 μl of PA aqueous solution and 50 μl of bFGF solutions (at concentrations of 0.04, 0.2, 0.6, and 1 $\mu\text{g}/\mu\text{l}$) were carefully injected separately at the same time into the back subcutis of male mice. At 1, 3, 7, 10, 14, 21, and 28 days post-treatment, the mice were sacrificed ($n = 6$ for each time point) by an overdose injection of anesthetic and the skin including the injected site ($2 \times 2\text{ cm}^2$) was carefully taken off for the

subsequent biological examinations. Photographs of the skin flaps were taken to record tissue appearance around the treated site.

Angiogenesis induced at the injected site was assessed in terms of histological and biochemical parameters. The angiogenesis of bFGF was estimated by determining the amount of tissue hemoglobin as a marker of angiogenesis [16]. Briefly, the tissue around the injected site of bFGF was scraped using a scalpel and immersed in 17 mM Tris–HCl buffer solution (pH 7.6) containing 0.75% of ammonium chloride for 24 h at 4 °C to extract hemoglobin from the tissue. The extracted hemoglobin was quantitated using a hemoglobin assay kit (Wako Pure Chemicals Co. Ltd., Kyoto, Japan) based on a calibration curve which had been prepared by hemoglobin standard solutions.

For histological evaluation, the skin flaps were cut at the central portion of injected site by a scalpel. One cut of the skin was fixed with 10% neutralized formalin solution, embedded in paraffin, and sectioned (2 mm in thickness), followed by staining with hematoxylin and eosin (HE). Photomicrographs of three cross sections from different mice were taken at different magnifications to evaluate histologically vascularization.

In order to evaluate the vascularity in injection site, the explanted subcutis tissues were processed for immunohistological staining evaluation. After being rinsed with PBS three times, the samples were subjected to a FITC-conjugated mouse anti-smooth muscle α -actin (NeoMarkers), RODAMIN-conjugated mouse monoclonal anti-CD31 (Santa Cruz Cio) antibody, as endothelial marker, as well as DAPI to stain nucleus. This was followed by TRITC-conjugated goat-anti mouse IgG at 37 °C for 1 h. Fluorescence imaging was performed with a Leica TCS-ST2 confocal microscope.

To analyze the capillary density, we randomly chose five fields (5 mm²) from the injection site. After treatment with HE, the density of capillaries

in each field was evaluated by counting vessels in the five randomly chosen unit areas (500 mm²) under ocular micrometers (Olympus).

2.8. Statistical analysis

All the data were statistically analyzed to express the mean \pm the standard deviation (SD) of the mean. Student's *t* test was performed and $p < 0.05$ was accepted to be statistically significant.

3. Results

3.1. Preparation and characterization of PA

Fig. 1A shows a schematic representation of PA. The molecule contains three distinct regions: a hydrophobic alkyl tail, a hydrophilic region containing glycine and alanine, and a charged head group containing glutamic acid and RGD. Fig. 1B shows the TOF-mass results of PA synthesized after purification by using HPLC. The exact molecular weight of PA is 1168.6. TOF-mass results indicate that the molecular weight of synthesized PA found to be 1169.557: $[M + H]^+$, where *M* is the molecular weight of synthesized PA. TOF-mass results clearly indicate that the purity of synthesized PA obtained through HPLC was more than 85%.

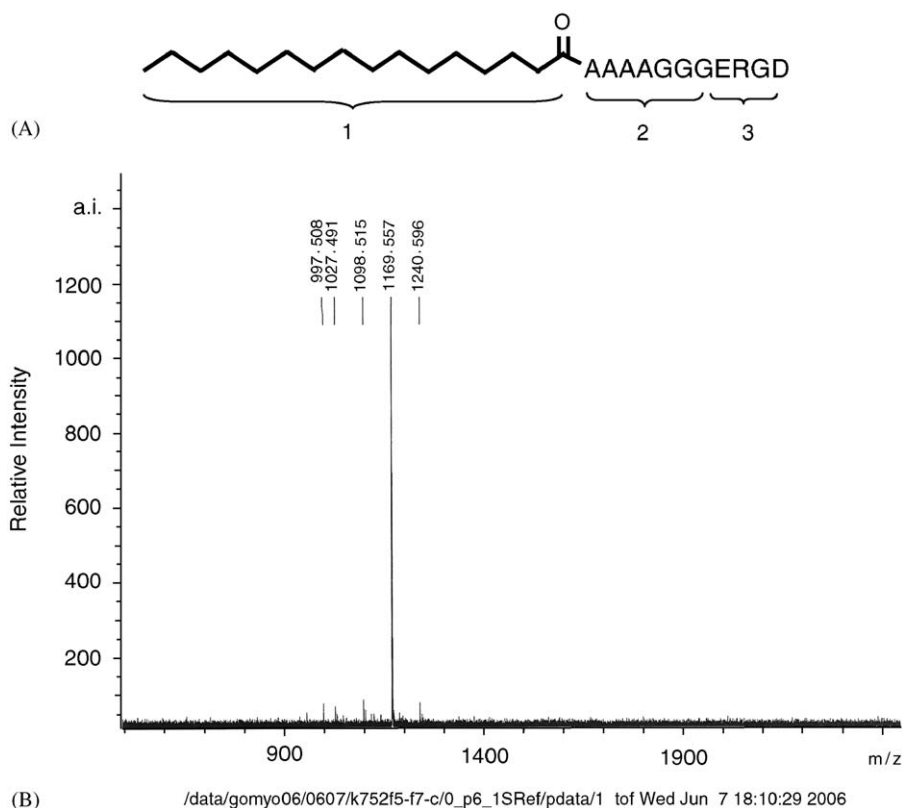


Fig. 1. Schematic representation of peptide amphiphile (A) and MALDI-TOF MS of synthesized PA after further purification by using HPLC (B). The molecule contains three distinct regions: Region 1 is a long alkyl tail that conveys hydrophobic character to the molecule and, when combined with the peptide region, makes the molecule amphiphilic. Region 2 is a flexible linker region of four alanine (A) and three glycine (G) to provide the hydrophilic head group flexibility from the more rigid cross-linked region. Region 3 is a charged head group containing a net negative charge of glutamic acid (E) and the cell adhesion ligand, arginine–glycine–aspartic acid (RGD).

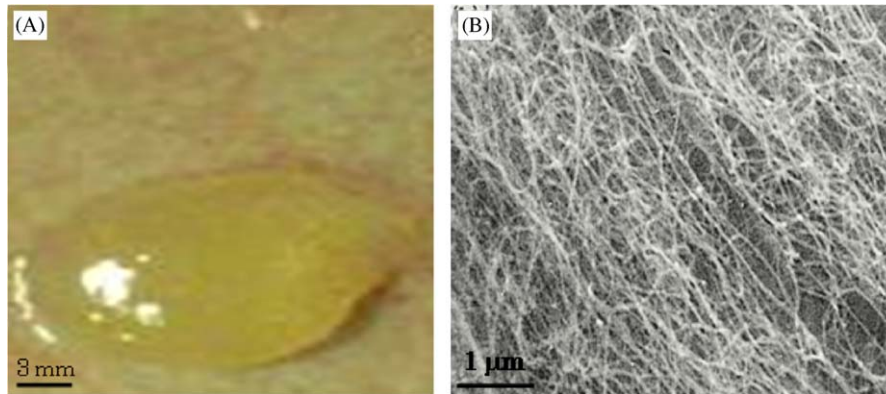


Fig. 2. Light microscopic photograph of a gel formed by adding bFGF solution to a PA aqueous solution (A) and SEM photograph of self-assembled PA nanofiber network (B). The concentration of bFGF used is $0.2 \mu\text{g}/\mu\text{l}$.

3.2. Morphology of self-assembled PA nanofibers

Fig. 2A shows the appearance of gel formed by adding of 1 wt% PA aqueous solution to bFGF solution in a 1:1 volume ratio. Fig. 2B shows SEM photograph of nanofibers formed through self-assembly of PA. SEM photograph of self-assembled PA revealed the formation of fibrous assemblies of nanofibers with an extremely high aspect ratio, and high surface areas.

3.3. In vitro release profile of bFGF

The amount of released bFGF from the self-assembled PA nanofibers as a function of time at pH = 7.4 is shown in Fig. 3. As shown, the release profile was characterized by an “initial burst” of protein during the first 10 h followed by a longer period (up to 750 h) of sustained release.

3.4. In vivo degradation of self-assembled PA nanofibers and in vivo release profile of bFGF

Fig. 4 shows the time course of self-assembled PA nanofibers and bFGF radioactivity remaining after subcutaneous injection of ^{125}I -labeled PA with bFGF and PA with ^{125}I -labeled bFGF. The remaining radioactivity of PA decreased with time, although the degradation time was slow and the PA was retained in the body over 28 days. On the other hand, the residual radioactivity of bFGF steeply decreased within 1 day of injection, but thereafter gradually decreased with time. The radioactivity following injection of only ^{125}I -labeled bFGF disappeared within 2 days.

3.5. Vascularization following treatment of bFGF with or without PA injection

Fig. 5 shows the tissue appearance, histological sections, and immunohistological staining of mouse subcutis 7 days after subcutaneous injection of PA solution, free bFGF, and bFGF injection with PA. A transparent gel was formed only after injection of bFGF with PA (Fig. 5C).

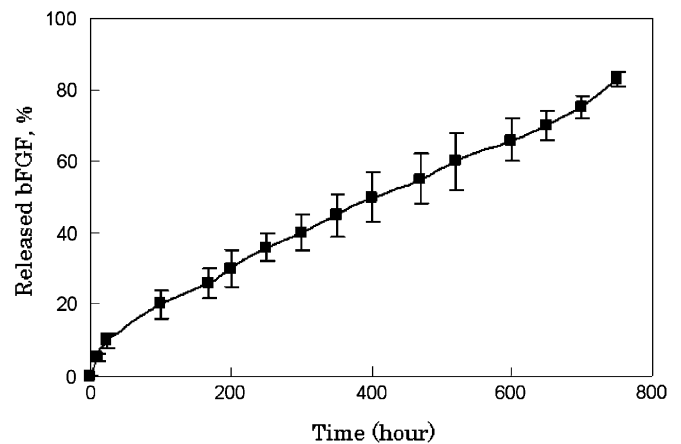


Fig. 3. In vitro bFGF release kinetic from self-assembled PA nanofibers. The concentration of bFGF used is $0.2 \mu\text{g}/\mu\text{l}$. $n = 6$, number of experiments for each time point.

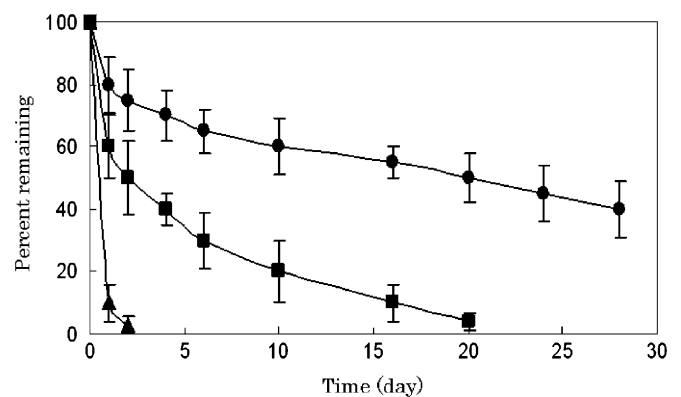


Fig. 4. Time course of radioactivity remaining of ^{125}I -labeled PA and ^{125}I -labeled bFGF after subcutaneous injection of free ^{125}I -labeled bFGF (▲), self-assembled PA nanofibers incorporating ^{125}I -labeled bFGF (■), and self-assembled ^{125}I -labeled PA nanofibers incorporating bFGF (●) into the back of mice. $n = 6$, number of mice used for each time point.

The injection of PA alone did not contribute in the formation of gel (Fig. 5A). Histological analysis revealed that when bFGF was injected together with PA solution,

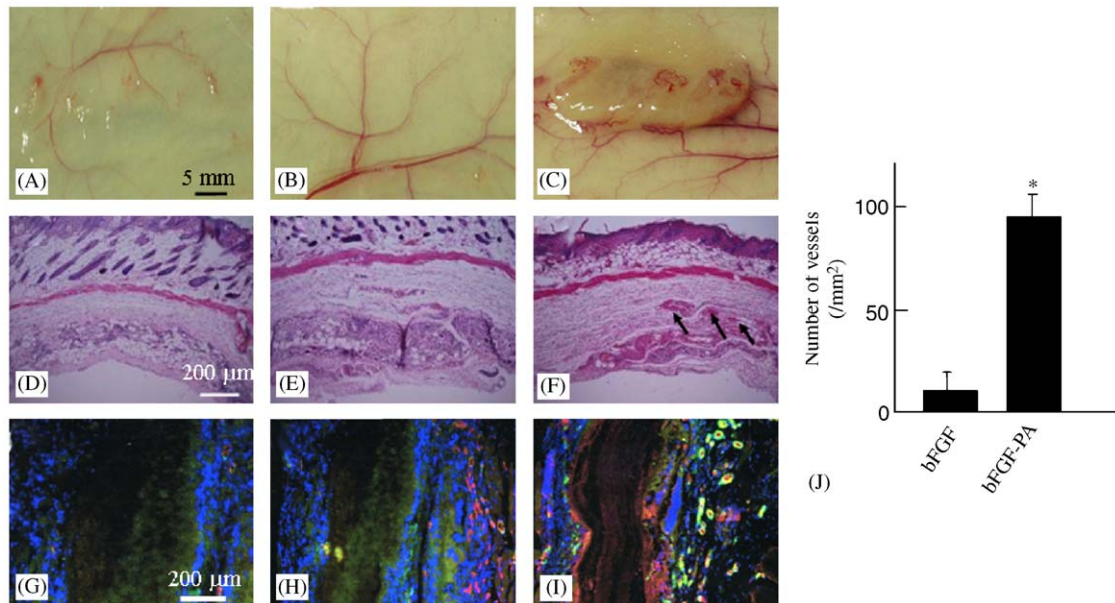


Fig. 5. Representative of tissue appearance (A, B, and C), histological sections (D, E, and F), and immunostaining (G, H, I) of mouse subcutis 7 days after subcutaneous injection of PA solution (A, D, and G), free bFGF solution (B, E, and H), and bFGF with PA (C, F, and I). Number of new vessels formed is shown in the right part as (J). The concentration of bFGF used is 0.2 μg/μl. The arrows in the histological sections indicate newly formed capillaries (Magnification: × 100, HE staining). Immunostaining indicates evidence of several capillaries in the injected site, where green: SMC α-actin, blue: nuclei, and red: CD31. * $p < 0.05$, significant against the value of group injected with free bFGF. $n = 6$, number of mice used for each group.

capillaries were newly formed at the injected site. The capillary density was significantly higher when bFGF was incorporated to PA as shown in Fig. 5F. This was confirmed by immunofluorescence staining for smooth muscle (SM) α-actin as well as for CD31. In order to test whether control released of bFGF contributed to angiogenesis, immunofluorescence analysis was performed. As shown in immunofluorescence staining, green staining indicate smooth muscle cells of capillaries wall and red staining indicates CD31 positive cells that indicates endothelial cells of vessels wall. Blue staining represents nucleuses. The number of smooth muscles cells of capillaries wall as well as endothelial cells of vessels wall greatly enhanced when release of bFGF was controlled by PA. Right graft (Fig. 5J) indicates that the number of vessels in bFGF incorporated PA was highest than that of free bFGF. We suggested that controlled release of bFGF from injectable PA enhanced angiogenesis.

Fig. 6 shows the time course of angiogenesis induced by free bFGF, PA solution, and bFGF injection with PA. The injection of bFGF solution did not increase the amount of hemoglobin at the injection site over the time range studied and the amount of tissue hemoglobin was similar to that of PA solution alone or untreated, normal mice. However, the injection of bFGF together with PA solution induced significant angiogenesis. The amount of tissue hemoglobin notably increased within 1 day of injection and the significantly increased level was retained over 28 days.

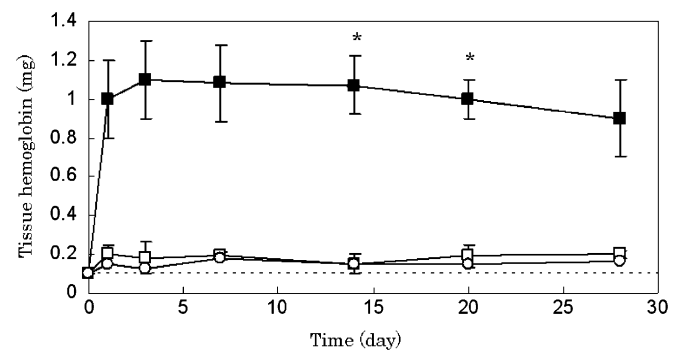


Fig. 6. Time course of neovascularization induced by subcutaneous injection of bFGF alone (□), PA (○), and bFGF with PA (■). The concentration of bFGF used is 0.2 μg/μl. The dotted line indicates the amount of tissue hemoglobin in the corresponding area of untreated, normal mice. * $p < 0.05$, significant against the value of group injected with bFGF. $n = 6$, number of mice used for each time point.

3.6. Effect of the bFGF dose on angiogenesis

Fig. 7 shows the effect of the bFGF dose on the angiogenesis induced by bFGF and bFGF with PA injection. Injection of bFGF solution alone did not increase the hemoglobin amount even though the highest dose of bFGF was injected and the level of tissue hemoglobin was similar to that of bFGF injection alone. On the contrary, the injection of bFGF together with PA resulted in a significant increase in the amount of tissue hemoglobin and an enhanced angiogenesis was observed when the bFGF dose was 0.2 μg/μl or higher.

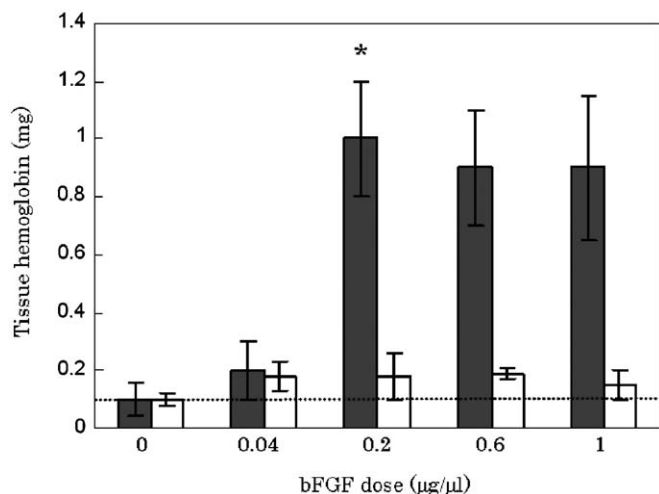


Fig. 7. Effect of the bFGF dose on the neovascularization induced by subcutaneous injection of bFGF alone (\square) and bFGF with PA (\blacksquare). The tissue hemoglobin was evaluated 7 days after subcutaneous injection. The dotted line indicates the amount of tissue hemoglobin in the corresponding area of untreated, normal mice. * $p < 0.05$, significant against the value of group injected with free bFGF. $n = 6$, number of mice used for each group.

4. Discussion

Efficient vascularization of tissue-engineered scaffolds is crucial for a successful tissue-engineering application. The use of angiogenic factors is a popular approach to induce neovascularization. Among them, bFGF plays a multifunctional role in stimulation of cell growth and tissue repair. However, it has a very short half-life when injected and is unstable in solution. To overcome these problems, bFGF was encapsulated within alginate, gelatin, agarose/heparin, collagen, and poly(ethylene-co-vinyl acetate) carriers [9,17,18]. According to the results of these studies, it is conceivable to incorporate the angiogenic factor to a sustained releasing system prior to the implantation.

The bFGF incorporated these releasing system requires surgery for implantation, which is not welcomed. We report here on solid scaffolds that incorporate bFGF and form by self-assembly from aqueous solutions of peptide amphiphiles. The scaffold consists of nanofiber networks formed by the aggregation of the amphiphilic molecules, and this process is triggered by the addition of bFGF suspensions to the aqueous solutions. The scaffolds formed by these systems could be delivered to living tissues by simply injecting a liquid (i.e., peptide amphiphile solutions) and bFGF solution. The injected solutions would form a solid scaffold at the injected site of tissue.

In vitro release profile indicates that the prolonged release of bFGF is continued for 750 h. When the release was halted, approximately 90% of total loaded protein had been released. However, it is possible to increase the cumulative amount of released molecules by increasing the

concentration of the loading solution because the amount of loaded protein may be increased as the concentration of loading solution increases. This result is attributed to an increasing driving force, i.e., concentration difference for protein diffusion. However, the type of interaction forces acting between bFGF and PA molecules is not clear at present.

In vivo degradation rate of self-assembled PA nanofibers and in vivo release profiles of bFGF were estimated in terms of the radioactivity loss of ^{125}I -labeled PA and ^{125}I -labeled bFGF. Therefore, injection of radioiodinated PA and bFGF into the mouse subcutis was carried out to evaluate the time profile of radioactivity remaining in vivo. As shown in Fig. 4, the PA was degraded with time in the body although the degradation rate was slow. The radioactivity of self-assembled PA nanofibers incorporating ^{125}I -labeled bFGF decreased with time although the bFGF radioactivity was retained for longer time periods than that of free ^{125}I -labeled bFGF injection. The decrement order and pattern of bFGF and PA radioactivity (Fig. 4) reveals that the in vivo release rate of bFGF was faster than the in vivo degradation rate of PA. Taken together, the results of in vitro and in vivo release profile indicate that bFGF was released from self-assembled PA nanofibers in the body as a result of combination of diffusion and degradation mechanism.

The bFGF used here was originally characterized in vitro as a growth factor for fibroblasts and capillary endothelial cells and in vivo as a potent mitogen and chemoattractant for a wide range of cells. In addition, bFGF is reported to have a variety of biological activities [19–21] and to be effective in enhancing wound healing through induction of neovascularization [22,23] and regeneration of bone [24,25], cartilage [26,27] and nerve [28,29], when administrated in the form of a solution. The most important of concern regarding the delivery of proteins is whether or not the protein released in the body actually retains its biological activity. To evaluate protein activity, in vitro culture techniques are normally employed because of their simplicity and convenience, compared with in vivo animal experiments. However, any in vitro non-degradation system cannot be applied to evaluate the biological activity of released bFGF. Thus, to obtain information on the retention of bFGF activity, we directly assessed vascularization after subcutaneously injection of PA with bFGF in animals. Fig. 5 clearly indicates that subcutaneous injection of bFGF together with PA was effective in enhancing bFGF-induced angiogenesis. Histological examination demonstrated that vascularization was remarkable around the injection site of self-assembled PA nanofibers incorporated bFGF, in contrast to sites injected with an aqueous solution of bFGF. Injection of bFGF in the form of a solution was not effective in inducing vascularization at all and injection of bFGF-free PA alone did not induce any vascularization effect. This was in good accordance with the results of immunofluorescence analysis. The number of smooth muscles cells of capillaries wall

as well as endothelial cells of vessels wall greatly enhanced when release of bFGF was controlled by PA. The prolonged period of angiogenesis by the bFGF-incorporated self-assembled PA nanofibers shown in Fig. 6, is ascribed to the prolonged time period of bFGF release. The amount of tissue hemoglobin, which is a measure of bFGF-induced neovascularization, notably increased within 1 day of injection of PA together with bFGF and the increased level was retained for several days, followed by a slow return over the time ranged studied. On the other hand, injection of an aqueous solution containing the same dose of bFGF, as a bFGF incorporated in self-assembled PA nanofibers, did not increase the amount of hemoglobin at the injection site over the time range studied; the level of tissue hemoglobin remained at approximately the same level as that found on injection of bFGF-free PA or in untreated mice (Fig. 6). No increase in the amount of hemoglobin was observed even when the amount of bFGF in solution that was injected was increased to 10 $\mu\text{g}/\mu\text{l}$ (data are not shown). This must be due to a rapid elimination of bFGF from the injection site. In contrast, the bFGF incorporated in self-assembled PA nanofibers enabled us to reduce the dose that was effective in inducing significant vascularization to 0.2 $\mu\text{g}/\mu\text{l}$. This finding strongly suggests that the bFGF-incorporated self-assembled PA nanofibers still maintain its biological activity even though exposed to an in vivo environment. It is highly possible that the slow degradation of the bFGF-incorporated self-assembled PA nanofibers achieves a longer period of bFGF release, resulting in a prolonged angiogenesis effect. The in vivo degradation profile of self-assembled PA nanofibers indicates that the retention period of the self-assembled PA nanofibers-induced vascularization effect was shorter than the degree of degradation of PA. As described earlier, bFGF seems to be released from self-assembled PA as a result of diffusion mechanism. The enhanced vascularization is due to the sustained release of bFGF.

5. Conclusion

The bFGF-incorporated PA developed in this study was found to be useful for prolonged growth factor release. As a flexible delivery system, these scaffolds can be adapted for sustained release of many different biomolecules. Also, both in vitro and in vivo studies proved that biocompatible self-assembled PA nanofibers is especially designed as a supporting prevascularization system. Incorporation of other angiogenic molecules such as VEGF and cell seeding into the matrix is currently under investigation. These results strongly suggest that the angiogenesis in advance induced by the controlled release of bFGF from bFGF-incorporated PA played an important role in creating an environment suitable for the survival and activity of transplanted cells for further applications in tissue regeneration.

Acknowledgments

This study was performed through Special Coordination Funds for Promoting Science and Technology from the MEXT, Japan, and partially supported by the Research Promotion Bureau (No. 16-794), MEXT, Japan.

References

- [1] Colton CK. Implantable biohybrid artificial organs. *Cell Transplant* 1995;4:415–36.
- [2] Polverini PJ. The pathophysiology of angiogenesis. *Crit Rev Oral Biol Med* 1995;6:230–47.
- [3] Ware JA, Simons M. Angiogenesis in ischemic heart disease. *Nat Med* 1997;3:158–64.
- [4] Thompson JA, Anderson KD, Dipietro JM, Zwiebel JA, Zametta M, Anderson WF, et al. Site-directed neovessel formation in vivo. *Science* 1988;241:1349–52.
- [5] Tabata Y, Nagano A, Ikada Y. Biodegradation of hydrogel carrier incorporating fibroblast growth factor. *Tissue Eng* 1999;5:127–38.
- [6] Tabata Y, Ikada Y. Vascularization effect of basic fibroblast growth factor released from gelatin hydrogels with different biodegradabilities. *Biomaterials* 1999;20:2169–75.
- [7] Cai S, Liu Y, Shu XZ, Prestwich GD. Injectable glycosaminoglycan hydrogels for controlled release of human basic fibroblast growth factor. *Biomaterials* 2005;26:6054–67.
- [8] Dogan AK, Gumusderelioglu M, Aksoz E. Controlled release of EGF and bFGF from dextran hydrogels in vitro and in vivo. *J Biomed Mater Res B Appl Biomater* 2005;74:504–10.
- [9] Edelman ER, Mathiowitz E, Langer R, Klagsburn M. Controlled and modulated release of basic fibroblast growth factor. *Biomaterials* 1991;12:619–26.
- [10] Ma Z, Kotaki M, Inai R, Ramakrishna S. Potential of nanofiber matrix as tissue-engineering scaffolds. *Tissue Eng* 2005;11:101–16.
- [11] Smith LA, Ma PX. Nano-fibrous scaffolds for tissue engineering. *Colloids Surf B: Biointerfaces* 2004;10:125–31.
- [12] Hartgerink JD, Beniash E, Stupp SI. Self-assembly and mineralization of peptide-amphiphile nanofibers. *Science* 2001;294:1684–8.
- [13] Silva GA, Czeisler C, Niece KL, Beniash E, Harrington DA, Kessler JA, et al. Selective differentiation of neural progenitor cells by high-epitope density nanofibers. *Science* 2004;303:1352–5.
- [14] Fields GB, Noble RL. Solid phase peptide synthesis utilizing 9-fluorenylmethoxycarbonyl amino acids. *Int J Peptide Protein Res* 1990;35:161–214.
- [15] Greenwood FC, Hunter WM, Gglover TC. The preparation of ^{131}I -labeled human growth hormone of high specific radioactivity. *Biochem J* 1963;89:114–23.
- [16] Kusaka M, Sudo K, Fujita T, Marui S, Itoh F, Ingber D, et al. Potent anti-angiogenic action of AGM-1470: comparison to the fumagillin parent. *Biochem Biophys Res Comm* 1991;174:1070–6.
- [17] Downs EC, Robertson NE, Riss TL, Plunkett ML. Calcium alginate beads as a slow release system for delivering angiogenic molecules in vivo and in vitro. *J Cell Physiol* 1992;152:422–9.
- [18] Iwakura A, Tabata Y, Tamura N, Doi K, Nishimura K, Nakamura T, et al. Gelatin sheets incorporating basic fibroblast growth factor enhances healing of devascularized sternum in diabetic rats. *Circulation* 2001;104(Suppl. 1):1325–9.
- [19] Gospodarowicz N, Ferrara L, Schweigerer L, Neufeld G. Structural characterization and biological functions of fibroblast growth factor. *Endocr Rev* 1987;8:95–114.
- [20] Rifkin DB, Moscatelli D. Recent development in the cell biology of basic fibroblast growth factor. *J Cell Biol* 1989;109:1–6.
- [21] Gospodarowicz N. Biological activities of fibroblast growth factor. *Ann NY Acad Sci* 1991;638:1–8.
- [22] Buntrock P, Jentzsch KD, Hender G. Stimulation of wound healing, using brain extract with fibroblast growth factor (FGF) activity. II.

- Histological and morphometric examination of cells and capillaries. *Exp Pathol* 1982;21:62–7.
- [23] McGee GS, Cavidson JM, Buckley A, Sommer A, Woodward SC, Aquino AM, et al. Recombinant basic fibroblast growth factor accelerates wound healing. *J Surg Res* 1988;45:145–53.
- [24] Rodan SB, Wesolowski KA, Thomas KA, Yoon K, Rodan GA. Effects of acidic and basic fibroblast growth factors on osteoblastic cells. *Connect Tissue Res* 1989;20:283–8.
- [25] Kawaguchi H, Kurokawa T, Hanada K, Hiyama Y, Tamura M, Ogata E, et al. Stimulation of fracture repair by recombinant human basic fibroblast growth factor in normal and streptozotocin-diabetic rats. *Endocrinology* 1994;135:774–81.
- [26] Cuevas P, Burgos J, Baird A. Basic fibroblast growth factor (FGF) promotes cartilage repair in vivo. *Biochem Biophys Res Commun* 1988;156:611–8.
- [27] Trippel SB. Growth factor actions on articular cartilage. *J Rheumatol* 1995;22:129–32.
- [28] Aebischer P, Salessiotis AN, Winn SR. Basic fibroblast growth factor released from synthetic guidance channels facilitates peripheral nerve regeneration across long nerve gaps. *J Neurosci Res* 1989;23:282–9.
- [29] Laquerriere A, Peulve P, Jin O, Tiollier J, Trady M, Vaurdy H, et al. Effect of basic fibroblast growth factor and α -melanocytic stimulating hormone on nerve regeneration through a collagen channel. *Microsurgery* 1994;15:203–10.